

AperTO - Archivio Istituzionale Open Access dell'Università di Torino

**TET1 is a tumour suppressor that inhibits colon cancer growth by derepressing inhibitors of the WNT pathway.**

**This is a pre print version of the following article:**

*Original Citation:*

*Availability:*

This version is available <http://hdl.handle.net/2318/150019> since 2016-08-12T10:55:30Z

*Published version:*

DOI:10.1038/onc.2014.356

*Terms of use:*

Open Access

Anyone can freely access the full text of works made available as "Open Access". Works made available under a Creative Commons license can be used according to the terms and conditions of said license. Use of all other works requires consent of the right holder (author or publisher) if not exempted from copyright protection by the applicable law.

(Article begins on next page)



# UNIVERSITÀ DEGLI STUDI DI TORINO

***This is an author version of the contribution published on:***

*Questa è la versione dell'autore dell'opera:*

[Oncogene (2015) 34, 4168–4176 doi:10.1038/onc.2014.356; ]

***The definitive version is available at:***

*La versione definitiva è disponibile alla URL:*

[<http://www.nature.com/onc/journal/v34/n32/full/onc2014356a.html>]

# **TET1 is a tumour suppressor that inhibits colon cancer growth by derepressing inhibitors of the WNT pathway**

Francesco Neri <sup>1</sup>, Daniela Dettori <sup>1</sup>, Danny Incarnato <sup>1,3</sup>, Anna Krepelova <sup>1,3</sup>, Stefania Rapelli <sup>1,3</sup>, Mara Maldotti <sup>1</sup>, Caterina Parlato <sup>1</sup>, Panagiotis Paliogiannis <sup>4</sup>, and Salvatore Oliviero <sup>1,2\*</sup>

<sup>1</sup> Human Genetics Foundation (HuGeF), via Nizza 52, Torino, Italy.

<sup>2</sup> Dipartimento di Scienze della Vita e Biologia dei Sistemi, Università di Torino, via Accademia Albertina, 13, Torino, Italy.

<sup>3</sup> Dipartimento di Biotecnologie Chimica e Farmacia, Università di Siena. via Fiorentina 1, Siena, Italy.

<sup>4</sup> Dipartimento di Scienze Chirurgiche, Microchirurgiche e Mediche, Viale S. Pietro 43, Università di Sassari, Sassari, Italy.

\* correspondence to :

Salvatore Oliviero Email : [salvatore.oliviero@hugef-torino.org](mailto:salvatore.oliviero@hugef-torino.org)

## **Abstract**

Ten eleven translocation (TET) enzymes catalyse the oxidative reactions of 5-methylcytosine (5mC) to promote the demethylation process. The reaction intermediate 5-hydroxymethylcytosine (5hmC) has been shown to be abundant in embryonic stem cells and tissues, but strongly depleted in human cancers. Genetic mutations of *TET2* gene were associated with leukaemia, whereas *TET1* downregulation has been shown to promote malignancy in breast cancer. Here, we report that *TET1* is downregulated in colon tumours from the initial stage. *TET1* silencing in primary epithelial colon cells increase their cellular proliferation while its re-expression in colon cancer cells inhibits their proliferation and the growth of tumour xenografts even at later stages. We found that *TET1* binds and maintains hypomethylated the promoter of the *DKK* genes inhibitors of the WNT signalling. Downregulation of *TET1* during colon cancer initiation leads to repression, by DNA methylation, the promoters of the inhibitors of the WNT pathway resulting in a constitutive activation of the WNT pathway. Thus the DNA hydroxymethylation mediated by *TET1* controlling the WNT signalling is a key player of tumour growth. These results provide new insights for understanding how tumours escape cellular controls.

## Introduction

DNA methylation plays essential role in the remodelling of the chromatin structure during development and tissue differentiation<sup>1-5</sup>. Deficient DNA methylation establishment, due to mutation in DNA methyltransferases Dnmt3a or Dnmt3b, can lead to genetic diseases, such ICF syndrome, and differentiation-associated methylation patterns are found altered in the majority of human cancers<sup>6-10</sup>. Irregular DNA methylation patterns are often associated with the tumour cells, where a general hypomethylation takes place together with hypermethylation of specific regions<sup>7,9,11-13</sup>. Colon cancer is one of the most susceptible disease to the deregulation of DNA methylation and often the tumour initiation is due to genetic mutation accomplished by epigenetic inactivation of the WNT pathway inhibitors<sup>10,14-16</sup>.

5-hydroxymethylcytosine (5hmC) is a recently discovered epigenetic modification catalysed by the Ten eleven translocation (TET) proteins that mediate the sequential oxidation of 5-methylcytosine (5mC) to 5hmC, leading to eventual DNA demethylation<sup>17-21</sup>. 5hmC is lost in human cancers, but the functional significance of this event is not still understood<sup>22-25</sup>. Several mechanisms can lead to loss of 5hmC in cancers, including mutations in IDH or TET2 genes<sup>26-29</sup>. Reduced levels of 5hmC, associated with mutations or reduced expression of *TET* genes, have been implicated in myeloproliferative disorders<sup>22-25,29-34</sup>. Downregulation of *TET1* has been shown to promote cancer invasion and metastasis<sup>35,36</sup>. Here we show that TET1 downregulation is not only linked to tumour progression and malignancy, but it is necessary for tumour initiation and growth. We reveal the molecular function of TET1 protein in cancer development and clarify the mechanism by which the WNT pathway inhibitors are epigenetically switched off during cellular transformation. This mechanism provides the explanation for specific promoter hypermethylations in cancer, which are TET-dependent, whereas a general hypomethylated state could

be caused by deregulation of the DNA methyltransferase machinery.

## Results

### ***TET1* downregulation is an early event in cell transformation**

We analysed the level *TET1* and hydroxymethylation in colon tumours. We found that *TET1* and 5hmC are strongly reduced in primary colon cancers with respect to the surrounding healthy tissue (Figure 1a and b). Interestingly, in our samples *TET1* was downmodulated independently from the tumour stage and the histopathological grade (Supplementary Figure S1a). To understand how *TET1* is regulated in tumours with respect in tumour initiation and progression, we analysed a metadataset from stages I to IV of colon, breast, lung, and rectum primary tumours. Analysis of the genes differentially expressed in this cohort of 887 adenocarcinomas revealed that *TET1*, but not *TET2* or *TET3*, was strongly downregulated in tumours since stage I (Supplementary Figure S1b). These data demonstrate that *TET1* downregulation is an early event in tumorigenesis. Quantitative RT-PCR (RT-qPCR) analysis showed *TET1* expression in human colon tissues and in normal epithelial colon cells (CCD), which were positive for the 5hmC modification, while *TET1* and 5hmC modification were almost undetectable in all the analysed colon cancer cell lines (Figure 1c and d). To understand *TET1* functional role in colon cells we silenced *TET1* in the normal CCD cells using two different short hairpin RNAs (shRNAs) (Figure S2a). *TET1*-knockdown CCD cells showed an increase in cell proliferation (Figure S2b) suggesting that *TET1* plays a role in the control of cell growth. To perform a rescue experiment we silenced *TET1* using the two shRNA together to increase the knockdown efficiency and re-expressed *TET1* by using a

cDNA missing its 3' UTR. TET1 re-expression in TET-silenced cell induced a full recovery of the level of 5hmC as well as a reduction of the cell proliferation rate (Figure 1e-g).

### ***TET1 blocks colon cancer cell growth *in vitro* and *in vivo****

The above results show that *TET1* is downregulated in colon cancers and that its downregulation in normal cells promotes cell proliferation. Next, we analysed the effects of *TET1* re-expression on the growth of colon cancer cells. To this end we first generated Caco-2 and SW48 human colorectal carcinoma cell lines stably expressing *TET1* under the control of a doxycycline-inducible (Dox) promoter (Figure 2a). *TET1* expression did not alter TET2 or TET3 expression (Supplementary Figure S3a and b). Upon cell treatment with Dox, TET1 induced an increased level of 5hmC and strongly reduced the growth rate of both cell lines (Figure 2b and c). These effects were due to the enzymatic activity of TET1, which lengthens the G0/G1 phase of the cell cycle while the hydroxylase deficient mutant TET1-H1672Y/D1674A (TET1-mut) was not able to interfere with cell growth *in vitro* (Supplementary Figure S3 c-f). Since both Caco-2 and SW48 form spheres under serum-free conditions (Supplementary Figure S4a and b) we also tested the effect of *TET1*-dependent hydroxymethylation on tumour initiating cells. *TET1* induction caused a significant reduction of sphere formation (Figure 2d). We analysed the surface markers CD166, CD44, and EpCAM that increase during sphere growth<sup>37</sup> but we did not observe any changes of these markers in Caco-2 or SW48 cells after TET1 re-expression suggesting that TET1 decreases cell proliferation independently from the cell fraction source and that it does not favor the proliferation of any particular fraction (Figure S4c).

To evaluate whether *TET1* plays a role in tumour growth *in vivo* we injected the

Caco-2 and SW48 cell lines in nude mice. A group of animals were then treated with Dox to induce the expression of *TET1* (Figure 3a). The size and weight of xenografts expressing *TET1* were dramatically smaller than the control group in which *TET1* was not induced (Figure 3b, c, and d, and Supplementary Figure S5a). *TET1* expression blocked the growth of the tumours derived from both cell lines from the beginning (Figure 3b). Remarkably, growth arrest was obtained not only when *TET1* was induced early after tumour cells inoculation but also when *TET1* was induced when the tumours were already established several days later (Figure 3e and Supplementary Figure S5b). These results are consistent with the strong inhibition of cell growth observed *in vitro*.

#### ***TET1* inhibits WNT signalling pathway**

To understand the molecular function of *TET1* expression on colon cancer, we performed a genome-wide RNA-Seq analysis of the mRNA of Caco-2 cells treated for 96h with doxycycline. This analysis revealed that *TET1* alters the expression of about 300 genes of which more than 60% were upregulated (Figure 4a). Interestingly, analysis of the genome-wide methylation pattern of wild type Caco2 cells<sup>38</sup> showed that the genes upregulated by *TET1* were those that exhibited a significant higher methylation level on their promoters (Figure 4b). Gene ontology analysis showed a significant enrichment in the WNT/ $\beta$ -catenin signalling pathway (p-value < 0.001) of the *TET1*-deregulated genes and many of them are involved directly or indirectly to the canonical WNT pathway (Figure 4c and d). We measured the level of nuclear  $\beta$ -catenin (*CTNNB1*) and we observed its reduced nuclear localization after *TET1* re-expression in both cancer cell lines (Figure 4e and f). We then analysed the effect of *TET1* expression on the WNT/ $\beta$ -catenin signalling pathway by using the TCF/LEF-dependent luciferase reporter assay since these cancer cells show high activity of this pathway (Supplementary Figure S6a). *TET1*



induced a downregulation of WNT/ $\beta$ -catenin signalling in both cell lines (Figure 4g). Also in this case, the enzymatic activity of *TET1* was required to downmodulate the WNT pathway activity (Supplementary Figure S6b). To demonstrate that the decreased proliferation rate was due to the *TET1*-dependent inactivation of the WNT pathway, we expressed a stable nuclear  $\beta$ -catenin in the Caco-2 and SW48 lines treated with Dox (Figure 4h). The expression of  $\beta$ -catenin in these cells rescued the luciferase activity and the cell growth (Figure 4i and Supplementary Figure S6c) demonstrating that the *TET1*-induced block of cell proliferation acts via WNT pathway inhibition. Interestingly, immunofluorescence analysis and Western blot of nuclear extracts of 24 days old xenografts showed sustained  $\beta$ -catenin nuclear localization in untreated but not in Dox treated mice (Figure S6d and e) indicating that also *in vivo* occurs a reduced WNT pathway activity in *TET1* expressing tumours.

### ***TET1*-dependent demethylation promotes transcriptional activation of the WNT pathway inhibitors**

RNA-Seq analysis showed proliferation-associated genes downregulated in *TET1* expressing Caco-2 cells, such as *MYC* and *Cyclin D2 (CCND2)* that are downstream targets of the WNT pathway. Importantly, *DKK* and *SFRP* genes, that are upstream inhibitors of the WNT pathway, were found upregulated in *TET1* expressing cells (Figure 5a). RT-qPCR analysis at 96 hours after Dox treatment showed the upregulation of *DKK3* and *DKK4* and the downregulation of *MYC* and *Cyclin D2* in both the cell lines (Figure 5b). Chromatin Immunoprecipitation (ChIP) analysis showed the binding of *TET1* on the promoters of *DKK* genes (Figure 5c). Analysis of the level of 5hmC and 5mC revealed a significant increase of 5hmC on the *DKK3* and *DKK4* genes associated with a reduction of 5mC signal (Figure 5d

and e). Interestingly, *DKK1* and *DKK2* expression was not affected by *TET1* (Figure 5b). *DKK1* was not methylated suggesting that on this gene the transcriptional repression is not mediated by DNA methylation. *DKK2* showed an elevated level of DNA methylation, which was not significantly reduced by *TET1* expression at 96 hours after Dox treatment (Figure 5e). To demonstrate that TET1 functions via repressing of the WNT inhibitors we performed a rescue experiment in which we silenced the *DKK3* and *DKK4* genes and re-expressed TET1 in Caco-2 and SW48 cells (Figure 5f). We used two different shRNAs to perform the knockdown of each *DKK* gene. The knockdown of both *DKK3* and *DKK4* restored the cell growth inhibition by TET1 expression (Figure 5g). Interestingly, RT-qPCR analysis of Caco-2 and SW48 tumour xenografts at later time points showed *DKK3* and *DKK4* upregulation as well as *MYC* and *Cyclin D2* downregulation (Figure S7). It is worth noting that the tumours expressed also *DKK2* (Figure S7), which was not upregulated within 96 hours of TET1 expression (Figure 5b) suggesting a cumulative *TET1*-dependent demethylation on the *DKK2* promoter in xenografts.

Taken together the above data demonstrate that TET1 inhibits cancer cells growth by repressing the WNT pathway, via demethylation of the promoters of the WNT inhibitors *DKK3* and *DKK4*.

## Discussion

We here demonstrate that TET1 loss in colon cancer is an early event that favours cell proliferation. We propose a model by which *TET1* downmodulation contributes to tumour initiation. Indeed, our data show that TET1 silencing in normal epithelial colon cells facilitates cell cycle progression and that its re-expression in transformed

colon cells blocks cell growth. Accordingly, meta-analysis on a cohort of 887 adenocarcinomas showed that *TET1* mRNA is downregulated from the first stage of tumours, especially in colon-rectal cancers. Thus the downmodulation of *TET1* takes place already at their initial stage suggesting that, in order to grow, cancer cells must downregulate *TET1* expression.

Our work demonstrated that TET1 downmodulation is required for cancer cell growth as its re-expression in cancer cells inhibits their growth both *in vitro* and *in vivo*. We found that *TET1* oncosuppressor function is mediated by its enzymatic activity, since the catalytically dead mutant was unable to block cancer cell growth.

The significant increase of 5hmC in TET1 expressing cells suggests that this modification could play gene regulatory functions in addition of being an intermediate for C-demethylation<sup>39,40</sup>

It has been previously shown in breast tissue that TET1 is required to maintain the expression of the antimetastatic miR200 and TIMP genes by inhibiting the methylation on their promoters and its downregulation in breast cancer results in the lower expression of these genes<sup>35,36</sup>. In contrast, in colon cancers, we could not find expression of miR200 or the downregulation of TIMP genes (data not shown). Instead, we found that TET1 targeting the *DKK* and *SFRP* genes induced a reduction of the 5mC and an increase of the 5hmC marks on their promoter regions leading to the expression of these genes.

Thus, in colon tumours the downregulation of the inhibitors of the WNT pathway, DKKs and SFRPs, due to *TET1* downmodulation, results in the increased of tumour growth. This implies that in different tissues, due to the cell-specific epigenetic landscape, cells respond with different phenotypic outputs to TET1 downmodulation. WNT pathway inhibitors *DKKs* and *SFRPs* are epigenetically inactivated by DNA methylation in colorectal cancer cells and this event is able to sustain tumour development<sup>14,15,41</sup>. Repression of these inhibitor genes allows a constitutive WNT signalling that sustains the proliferation of cancer cells. Our data demonstrate that

the gain of DNA methylation on these promoters is due to the reduced TET1-dependent demethylation activity.

In colon cancer cells, the loss of *TET1* promotes DNA methylation of these promoters leading to a full repression of the genes, which is revertible by *TET1* re-expression.

In summary, our data show that *TET1* acts as an oncosuppressor because it plays a central role in the epigenetic control of colon cancer growth. *TET1* reactivation, although challenging, can represent a novel therapeutic approach in cancer.

## **Material and methods**

### **Cell culture, transfection and transduction**

Caco2 and SW48 cells were cultured in RPMI medium with 10% FCS. For Doxycycline-inducible stable clone generation Caco2 and SW48 cells were transduced with 10  $\mu$ l of concentrated virus of pLVX-Tight-Puro-TET1 and pLVX-Tet-On-Advanced Vectors and selected for 7 days in Puromycin 1 mg/ml and Hygromycin B 100 mg/ml. For induction of TET1, Doxycycline was used at 1 mg/ml. Transfections were performed using Lipofectamine 2000 Transfection Reagent (Invitrogen) according to the manufacturer's protocol. CCD normal colon epithelial cells were acquired from ATCC (CCD 841 CoN (ATCC<sup>®</sup> CRL-1790<sup>™</sup>)) and cultured as described by ATCC. For shRNA transduction, 10  $\mu$ l of concentrated virus of PLKO vectors were incubated with cells for 16 hours.

### **Animals**

C57BL/6 mice (8-10 weeks old) were obtained from our mouse facility. BALB/c-nude (6 weeks old) were obtained from Janvier-labs. Housing and all experimental animal procedures were approved by the Institutional Animal Care and Research Advisory Committee of the University of Turin.

### **Constructs**

pAAV-EF1a-HA-hTet1CD-WPRE-PolyA and pAAV-EF1a-HA-hTet1CDmu-WPRE-PolyA were purchased from Addgene (plasmid 39454 and 39455). pLVX-Tight-Puro Vector and pLVX-Tet-On-Advanced Vector were purchased from Clontech (plasmid

S4934 and S4932). Catalytic domain of TET1 was sub-cloned into pLVX-Tight-Puro-Vector. TET1, DKK3 and DKK4 shRNAs were constructed using the TRC hairpin design tool (<http://www.broadinstitute.org/rnai/public/seq/search>) choosing the following hairpin sequences:

ACACAACCTTGCTTCGATAATT (TET1, shRNA1)

TTGTGCCTCTGGAGGTTATAA (TET1, shRNA2).

GACACGAAGGTTGGAAATAAT (DKK3, shRNA1)

GGCATGCACATCTGGAATTAA (DKK3, shRNA2).

TCGGCAGCATGCTCGATTAAG (DKK4, shRNA1)

GGAAGCCAAGTATTAAGAAAT (DKK4, shRNA2).

Annealed oligonucleotides were cloned into pLKO.1 vector (Addgene: 10878) and each construct was verified by sequencing. Super8X-TOPFlash, negative control Super8X-FOPFlash and pCS2-CTNNB1-S33A-myc-tag were kindly provided by Professor Valeria Poli.

## **Antibodies**

The antibodies were purchased from Millipore (anti-TET1), Abcam (anti-ssDNA), Cell Signalling (anti-CD44-8E2, anti-EpCAM), Sigma-Aldrich (anti-B-actin), Epitomics (anti-CD166), BD Transduction Laboratory (anti-CTNNB1), SantaCruz (anti-LaminA-sc20680), and Active Motif (anti-5mC, anti-5hmC).

## **DNA Extraction and dot-blot analysis**

Genomic DNA was extracted from cells using DNeasy Blood and Tissue kit (Qiagen). For dot-blot analysis, extracted genomic DNA was sonicated for 15 cycles

to obtain 300 bp fragments, denatured with 0.4 M NaOH and incubated for 10 min at 95°C prior to being spotted onto Hybond™-N+ (GE Healthcare). Membranes were saturated with milk 5% and incubated 16h with the specific antibodies.

### **RNA extraction and RT-PCR analysis**

RNA extraction and RT-PCR were performed as in <sup>42</sup>. Briefly, total RNA was extracted using TRIzol reagent (Invitrogen). Real-time PCR was performed using the SuperScript III Platinum One-Step Quantitative RT-PCR System (Invitrogen, cat.11732-020) following the manufacturer's instructions. Primers sequences are provided in Supplementary Table S1.

### **RNA sequencing**

For mRNA-Seq, libraries were generated from total RNA using TruSeq RNA Sample Preparation v2 in accordance to the manufacturer's protocol. Samples were sequenced on Illumina HiScanSQ platform. Reads were mapped on hg19 using TopHat v2.0.6 <sup>43</sup> and mRNA quantification was performed using Cuffdiff v2.0.2 <sup>44</sup>. Up- and down-regulated genes are provided in Supplementary Table S3. Raw data are deposited under the GEO accession GSE53172.

### **ChIP and (h)MeDIP**

ChIP were performed as in <sup>45</sup>. For MeDIP and hMeDIP, 2 µg of sonicated DNA was denatured at 95°C for 10 minutes, immediately cooled on ice for 10 minutes and diluted in 400 µl of IP buffer (10 mM Na-Phosphate pH 7.0 140 mM NaCl 0.05 %

Triton X-100) with 10 µl of anti-5mC or anti-5hmC. After incubation of 2 hours with at 4°C with overhead shaking, 30 µl of saturated Dynabeads anti-mouse IgG were added and incubate for other 2 hours. After five washes with IP buffer, DNA was eluted with Proteinase K for 2 hours and purified using the QIAQuick PCR Purification Kit (QIAGEN) according to the manufacturer's instructions. DNA was analyzed by quantitative real-time PCR by using a SYBR GreenER kit (Invitrogen). Primers sequences are provided in Supplementary Table S2.

### **Protein extraction and Western blotting**

Extracts were performed as previously described<sup>46</sup>. Briefly, cells were resuspended in F-buffer (10mM TRIS-HCl pH 7.0, 50mM NaCl, 30mM Na-pyrophosphate, 50mM NaF, anti-proteases) and sonicated for 3 pulses to obtain total cell extracts. Nuclear protein extraction was performed as in<sup>3</sup>. Extracts were quantified using bicinchoninic acid (BCA) assay (BCA protein assay kit; catalog no. 23225; Pierce) and were run in SDS-polyacrylamide gels at different percentages, transferred to nitrocellulose membranes and incubated 16 hours with specific primary antibodies.

### **Luciferase assay**

Cells were transfected with the indicated Firefly luciferase reporter constructs with 1/10 of Renilla Luciferase reporter construct. After 24 h cells were analyzed for luciferase and Renilla activity using a Dual-Glo luciferase assay (Promega). Promoter activity values were normalized using Renilla activity.

### **Immunofluorescence**



For immunostaining tumours were dissected and fixed in 2% PAF overnight at 4°C, dehydrated and embedded in paraffin. Thick sections (5 µm thickness) were then incubated with anti-CTNNB1 antibody.

### **Cell growth and cell cycle analysis**

For cell growth assay,  $5 \times 10^4$  cells were plated in 35mm wells and counted at the indicated time point using Scepter™ Automated Cell Counter (Millipore). For FACS cell cycle analysis, the cells were stained with propidium iodide (PI) solution (0.1% Triton, 200 mg/ml RNase, 20 mg/ml PI in PBS) for 30 min at room temperature. Acquisition was performed using Becton Dickinson FACS Canto and analysis was done with FACS FlowJo Software.

### **FACS analysis**

FACS analysis was performed as previously described (Neri *et al.*, 2012) Briefly, cells were first incubated with primary antibodies for 30 minutes in PBS-1% bovine serum albumin (BSA) and after 3 washes were stained with conjugated secondary antibodies.

### **Colonsphere assay**

Colonsphere assay was performed as in <sup>37</sup> with the following modifications: cells were plated as single cell in 96 well round bottom in DMEM/F12 medium supplemented with BSA 0.4%, Heparin 4mg/ml, Insulin 20mg/ml, B27, N2, bFGF 10ng/ml, EGF 20ng/ml and cultured for 10 days before analysis.

## **Mouse and tumours injection**

Caco2 and SW48 human colon tumour cell lines were harvested and single-cell suspensions of  $1 \times 10^6$  in 100  $\mu$ l of PBS were injected subcutaneously into the right flank of mice. Tumour volumes were measured every two days with a caliber using the formula:  $V = \pi \times [d^2 \times D] / 6$ , where d is the minor tumour axis and D is the major tumour axis. The mice were sacrificed at defined time intervals after cell inoculation or when tumours reached a maximum size of 2  $\text{cm}^3$ .

## **Bioinformatics analysis**

Gene expression analysis of TET1, TET2 and TET3 was performed using The Cancer Genome Atlas TCGA database (<http://cancergenome.nih.gov/>) subdividing the cancers for their reported tumour stage where it was available, otherwise the data were not used. Gene ontology was performed using DAVID software<sup>47,48</sup>

## **Conflict of interest**

All the other authors declare no conflict of interest.

## **Acknowledgement**

This work was supported by the Associazione Italiana Ricerca sul Cancro (AIRC) IG 2011/11982. We thank Carola Ponzetto and Riccardo Tauli for the critical reading of

the manuscript.

## References

1. Okano, M., Bell, D. W., Haber, D. A. & Li, E. DNA methyltransferases Dnmt3a and Dnmt3b are essential for de novo methylation and mammalian development. *Cell* **99**, 247–257 (1999).
2. Smith, Z. D. & Meissner, A. DNA methylation: roles in mammalian development. *Nat Rev Genet* **14**, 204–220 (2013).
3. Neri, F. *et al.* Dnmt3L antagonizes DNA methylation at bivalent promoters and favors DNA methylation at gene bodies in ESCs. *Cell* **155**, 121–134 (2013).
4. Bestor, T. H. The DNA methyltransferases of mammals. *Human Molecular Genetics* **9**, 2395–2402 (2000).
5. Lienert, F. *et al.* Identification of genetic elements that autonomously determine DNA methylation states. *Nat Genet* **43**, 1091–1097 (2011).
6. Bestor, T. H. *et al.* Chromosome instability and immunodeficiency syndrome caused by mutations in a DNA methyltransferase gene. *Nature* **402**, 187–191 (1999).
7. Jones, P. A. DNA methylation and cancer. *Oncogene* **21**, 5358–5360 (2002).
8. Rhee, J.-K. *et al.* Integrated analysis of genome-wide DNA methylation and gene expression profiles in molecular subtypes of breast cancer. *Nucleic Acids Research* **41**, 8464–8474 (2013).
9. Easwaran, H. *et al.* A DNA hypermethylation module for the stem/progenitor cell signature of cancer. *Genome Research* **22**, 837–849 (2012).
10. Rhee, I. *et al.* DNMT1 and DNMT3b cooperate to silence genes in human cancer cells. *Nature* **416**, 552–556 (2002).
11. Teng, I. W. *et al.* Targeted Methylation of Two Tumor Suppressor Genes Is Sufficient to Transform Mesenchymal Stem Cells into Cancer Stem/Initiating Cells. *Cancer Research* **71**, 4653–4663 (2011).
12. Gaudet, F. Induction of Tumors in Mice by Genomic Hypomethylation. *Science* **300**, 489–492 (2003).
13. Feltus, F. A., Lee, E. K., Costello, J. F., Plass, C. & Vertino, P. M. Predicting aberrant CpG island methylation. *Proc. Natl. Acad. Sci. U.S.A.* **100**, 12253–12258 (2003).
14. Sato, H. *et al.* Frequent epigenetic inactivation of DICKKOPF family genes in human gastrointestinal tumors. *Carcinogenesis* **28**, 2459–2466 (2007).

15. Suzuki, H. *et al.* Epigenetic inactivation of SFRP genes allows constitutive WNT signaling in colorectal cancer. *Nat Genet* **36**, 417–422 (2004).
16. Jin, B. *et al.* DNMT1 and DNMT3B Modulate Distinct Polycomb-Mediated Histone Modifications in Colon Cancer. *Cancer Research* **69**, 7412–7421 (2009).
17. Tahiliani, M. *et al.* Conversion of 5-methylcytosine to 5-hydroxymethylcytosine in mammalian DNA by MLL partner TET1. *Science* **324**, 930–935 (2009).
18. Ito, S. *et al.* Tet Proteins Can Convert 5-Methylcytosine to 5-Formylcytosine and 5-Carboxylcytosine. *Science* **333**, 1300–1303 (2011).
19. Maiti, A. & Drohat, A. C. Thymine DNA Glycosylase Can Rapidly Excise 5-Formylcytosine and 5-Carboxylcytosine: POTENTIAL IMPLICATIONS FOR ACTIVE DEMETHYLATION OF CpG SITES. *Journal of Biological Chemistry* **286**, 35334–35338 (2011).
20. He, Y. F. *et al.* Tet-Mediated Formation of 5-Carboxylcytosine and Its Excision by TDG in Mammalian DNA. *Science* **333**, 1303–1307 (2011).
21. Neri, F. *et al.* Genome-wide analysis identifies a functional association of Tet1 and Polycomb repressive complex 2 in mouse embryonic stem cells. *Genome Biol.* **14**, R91 (2013).
22. Haffner, M. C. *et al.* Global 5-hydroxymethylcytosine content is significantly reduced in tissue stem/progenitor cell compartments and in human cancers. *Oncotarget* **2**, 627–637 (2011).
23. Kudo, Y. *et al.* Loss of 5-hydroxymethylcytosine is accompanied with malignant cellular transformation. *Cancer Sci* **103**, 670–676 (2012).
24. Lian, C. G. *et al.* Loss of 5-hydroxymethylcytosine is an epigenetic hallmark of melanoma. *Cell* **150**, 1135–1146 (2012).
25. Yang, H. *et al.* Tumor development is associated with decrease of TET gene expression and 5-methylcytosine hydroxylation. 1–7 (2012). doi:10.1038/onc.2012.67
26. Bacher, U. *et al.* Mutations of the TET2 and CBL genes: novel molecular markers in myeloid malignancies. *Ann Hematol* **89**, 643–652 (2010).
27. Kudo, Y. *et al.* Tet2 Facilitates the Derepression of Myeloid Target Genes during CEBP $\alpha$ -Induced Transdifferentiation of Pre-B Cells. *Molecular Cell* 1–11 (2012). doi:10.1016/j.molcel.2012.08.007
28. Prensner, J. R. & Chinnaiyan, A. M. Metabolism unhinged: IDH mutations in cancer. *Nature Publishing Group* **17**, 291–293 (2011).
29. Hsu, C.-H. *et al.* The Oncogenic MicroRNA miR-22 Targets the TET2 Tumor Suppressor to Promote Hematopoietic Stem Cell Self-Renewal and Transformation. *Stem Cell* **13**, 87–101 (2013).
30. Jin, S. G. *et al.* 5-Hydroxymethylcytosine Is Strongly Depleted in Human Cancers but Its Levels Do Not Correlate with IDH1 Mutations. *Cancer Research* **71**, 7360–7365 (2011).
31. Li, W. *et al.* MicroRNA-Antagonism Regulates Breast Cancer Stemness and Metastasis via TET-Family-Dependent Chromatin Remodeling. *Cell* 1–22 (2013). doi:10.1016/j.cell.2013.06.026

32. Tefferi, A. *et al.* TET2 mutations and their clinical correlates in polycythemia vera, essential thrombocythemia and myelofibrosis. *Leukemia* **23**, 905–911 (2009).
33. Kosmider, O. *et al.* TET2 mutation is an independent favorable prognostic factor in myelodysplastic syndromes (MDSs). *Blood* **114**, 3285–3291 (2009).
34. Saint-Martin, C. *et al.* Analysis of the Ten-Eleven Translocation 2 (TET2) gene in familial myeloproliferative neoplasms. *Blood* **114**, 1628–1632 (2009).
35. Sun, M. *et al.* HMGA2/TET1/HOXA9 signaling pathway regulates breast cancer growth and metastasis. *Proc. Natl. Acad. Sci. U.S.A.* **110**, 9920–9925 (2013).
36. Hsu, C.-H. *et al.* TET1 Suppresses Cancer Invasion by Activating the Tissue Inhibitors of Metalloproteinases. *Cell Reports* **2**, 568–579 (2012).
37. Kanwar, S. S., Yu, Y., Nautiyal, J., Patel, B. B. & Majumdar, A. P. N. The Wnt/beta-catenin pathway regulates growth and maintenance of colonospheres. *Mol. Cancer* **9**, 212 (2010).
38. Wang, H. *et al.* Widespread plasticity in CTCF occupancy linked to DNA methylation. *Genome Research* **22**, 1680–1688 (2012).
39. Ivanov, M. *et al.* Ontogeny, distribution and potential roles of 5-hydroxymethylcytosine in human liver function. *Genome Biol.* **14**, R83 (2013).
40. Pfeifer, G. P., Kadam, S. & Jin, S.-G. 5-hydroxymethylcytosine and its potential roles in development and cancer. *Epigenetics & Chromatin* **6**, 10 (2013).
41. Aguilera, O. *et al.* Epigenetic inactivation of the Wnt antagonist DICKKOPF-1 (DKK-1) gene in human colorectal cancer. *Oncogene* **25**, 4116–4121 (2006).
42. Incarnato, D., Neri, F., Diamanti, D. & Oliviero, S. MREdictor: a two-step dynamic interaction model that accounts for mRNA accessibility and Pumilio binding accurately predicts microRNA targets. *Nucleic Acids Research* **41**, 8421–8433 (2013).
43. Kim, D. *et al.* TopHat2: accurate alignment of transcriptomes in the presence of insertions, deletions and gene fusions. *Genome Biol.* **14**, R36 (2013).
44. Trapnell, C. *et al.* Differential analysis of gene regulation at transcript resolution with RNA-seq. *Nat Biotechnol* **31**, 46–53 (2013).
45. Evellin, S. *et al.* FOSL1 controls the assembly of endothelial cells into capillary tubes by direct repression of  $\alpha$ v and  $\beta$ 3 integrin transcription. *Mol. Cell. Biol.* (2013). doi:10.1128/MCB.01054-12
46. Krepelova, A., Neri, F., Maldotti, M., Rapelli, S. & Oliviero, S. Myc and max genome-wide binding sites analysis links the myc regulatory network with the polycomb and the core pluripotency networks in mouse embryonic stem cells. *PLoS ONE* **9**, e88933 (2014).
47. Huang, D. W., Sherman, B. T. & Lempicki, R. A. Bioinformatics enrichment tools: paths toward the comprehensive functional analysis of large gene lists. *Nucleic Acids Research* **37**, 1–13 (2009).
48. Huang, D. W., Sherman, B. T. & Lempicki, R. A. Systematic and

integrative analysis of large gene lists using DAVID bioinformatics resources. *Nat Protoc* **4**, 44–57 (2008).

## Figure legends

### Figure 1.

Correlation between *TET1*/5hmC and (cancer) cell proliferation. **(a)** qRT-PCR of *TET1* mRNA in colon tumours samples and their relative healthy tissues. Error bars represent the standard deviation of 3 technical replicates. **(b)** Dot-blot analysis of 5hmC and 5mC in colon tumours samples and their relative healthy tissues. ssDNA was used as loading control. **(c)** qRT-PCR of *TET1* mRNA in the indicated cancer lines or primary cells. **(d)** Dot-blot analysis of 5hmC and 5mC in the indicated cancer lines or primary cells. ssDNA was used as loading control. **(e)** qRT-PCR of *TET1* mRNA in CCD normal human colon cells treated with a control shRNA, with two different shRNA against *TET1* or with two different shRNA against *TET1* plus *TET1* cDNA. **(f)** Dot-blot analysis of 5hmC and 5mC in CCD cells treated as in (e). ssDNA was used as loading control. **(g)** Cell growth assay in in CCD cells treated as in (e). Error bars represent the standard deviation of 3 independent experiments.

### Figure 2.

*TET1* regulates cancer cell proliferation. **(a)** Western Blot (WB) analysis of *TET1* in control or Doxycycline (Dox) treated Caco2 or SW48 colon cancer cell lines expressing inducible *TET1*. *ACTB* was used as loading control. **(b-c)** Dot-blot analysis of 5hmC and cell growth assay of wt or *TET1* inducible expressing ( $\pm$  Dox) Caco2 and SW48 cell lines. **(d)** Quantification of colonspheres obtained in colonspheres assay using the cell lines treated as in (c). Error bars represent the standard deviation of 3 independent experiments. (\* pvalue < 0.01)

**Figure 3.**

*TET1* inhibits cancer growth. (a) qRT-PCR of *TET1* mRNA in the indicated cell line xenografts after 3 weeks. (b) Mouse tumour growth of *TET1* inducible expressing ( $\pm$  Dox) Caco2 and SW48 cell line respectively. (c) Macroscopic view showing tumours upon resection from BALB/c-nude mice respectively of Caco2 and SW48 cell line implanted subcutaneously. (d) Tumours weight upon resection. (e) Reduced tumour growth of Caco2 and SW48 cell line by *TET1* expression upon post-implantation Doxycycline (Dox) treatment from the indicated day. Error bars in the Fig. represent the standard deviation of at least 3 independent experiments.

**Figure 4.**

*TET1* negatively regulates Wnt pathway in cancer cells. (a) Up- and down-regulated genes obtained from RNA-Seq analysis in Caco2 cell line expressing *TET1* for 96h. (b) Promoter methylation percentage of the up- and down-regulated gene in Caco2 after 96h. Promoter methylation was calculated using RRBS data from Encode (GSM980582) as the percentage of methylated CpGs in the region between -1000/+500 from TSS. (c) Gene Ontology (GO) analysis of deregulated genes in Caco2 cell line expressing *TET1* after 96h. (d) Schematic representation of the canonical WNT pathway with in red the up-regulated genes and in blue the down-regulated genes by *TET1* expression in Caco2 cell line. (e) WB analysis of CTNNB1 in nuclear (Nuc) or cytoplasmic (Cyt) extracts of Caco2 or SW48 cells treated with Dox at the indicated times. LAMIN A and ACTIN was used as loading control. (f) Nuclear localization loss of CTNNB1 in Doxycycline treated or untreated CACO-2 and SW48 cells for 48hours. DAPI is used for nuclei staining. (g) Caco2 and SW48 cells were transfected with a WNT-reporter (firefly TOP vector) and a Renilla luciferase (normalizing transfection control) constructs. The reporter activity was measured 24h after transfection in cells treated or not with Dox for 24h or 96h. (h) WB analysis of CTNNB1 in total extracts of Caco2 or SW48 cells treated with Dox and transfected with Mock or CTNNB1 (active form S33A). ACTB was used as loading control. i) Cell growth assay

in Mock or CTNNB1 transfected Caco2 and SW48 cells treated with Dox for *TET1* induction. Error bars in the Figure represent the standard deviation of 3 independent experiments.

**Figure 5.**

*TET1* derepresses WNT inhibitors. (a) Heatmap of the most regulated genes of the WNT pathway. (b) qRT-PCR of *DKKs*, *MYC* and *CCND2* mRNA levels in Caco2 and SW48 cell lines  $\pm$  Dox treatment. (c) ChIP analysis of the *DKK* gene promoters in Caco-2 and SW48 cells  $\pm$  Dox treatment. (d-e) (h)MeDIP analysis of *DKK* gene promoters in Caco-2 and SW48 cells  $\pm$  Dox treatment. (f) RT-qPCR of *DKK3* and *DKK4* in Caco2 and SW48 treated with Dox and transfected with control or *DKK3* and *DKK4* shRNAs. (g) Cell growth assay in Caco2 and SW48 cells treated as in (f). Error bars represent the standard deviation of 3 independent experiments. (\* pvalue < 0.01, \*\* pvalue < 0.05).



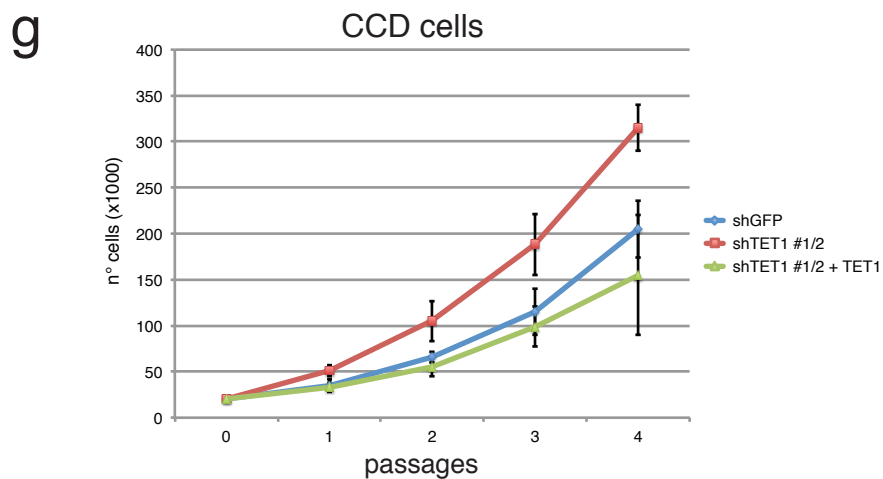
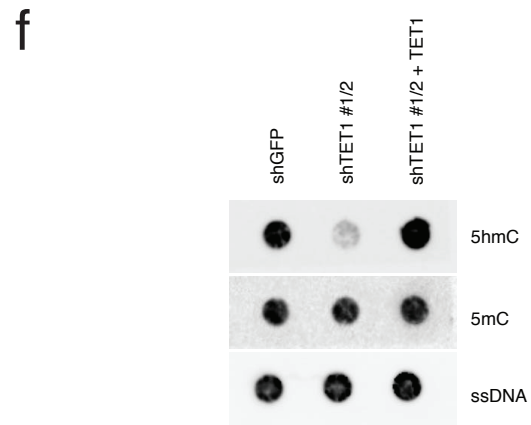
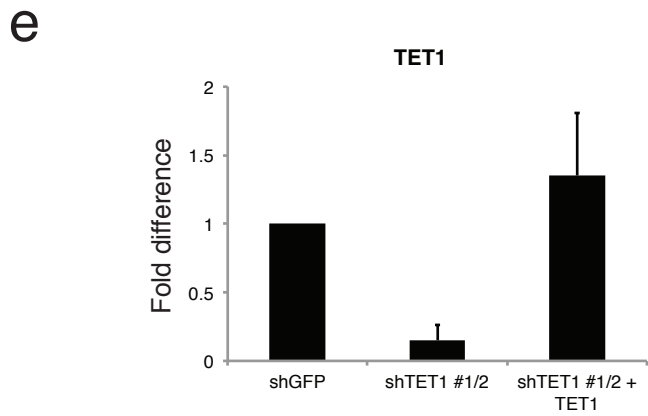
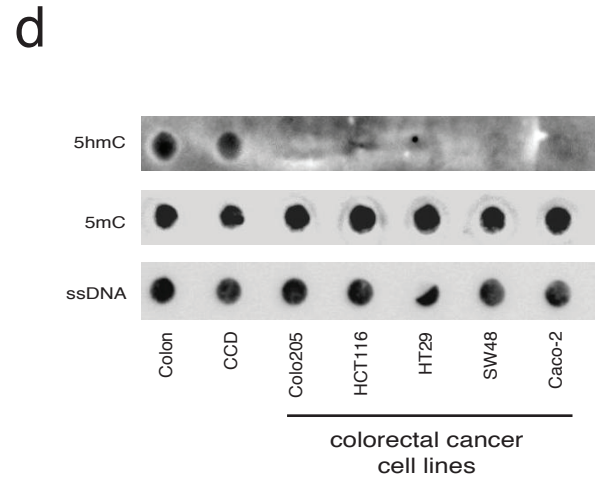
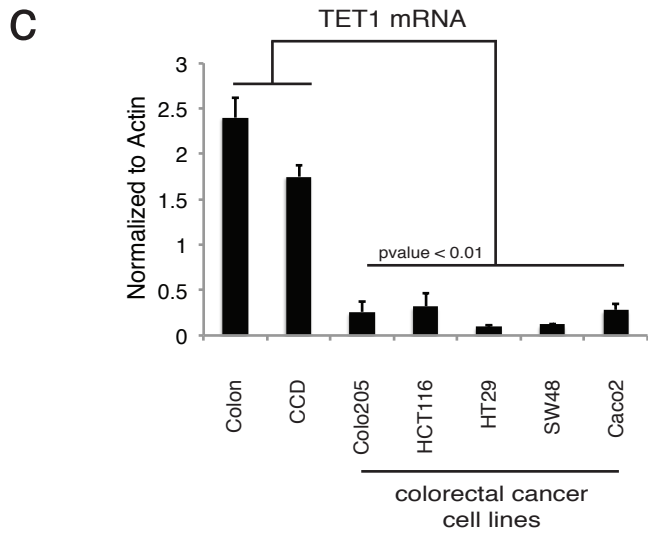
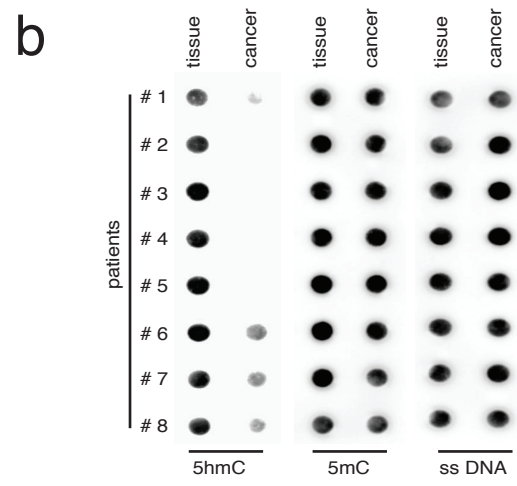
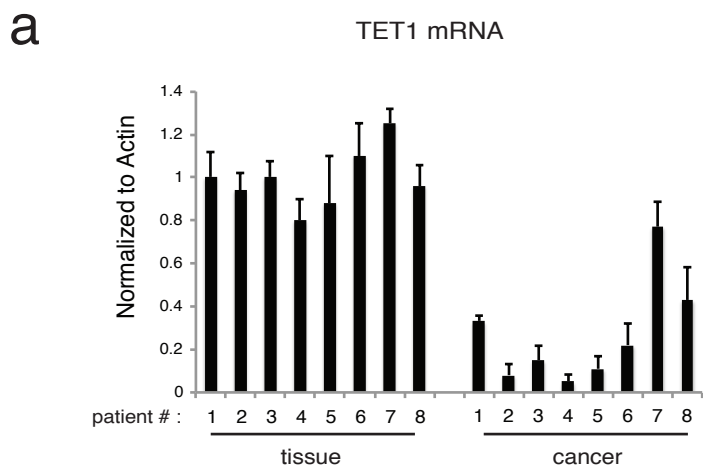


Figure 1

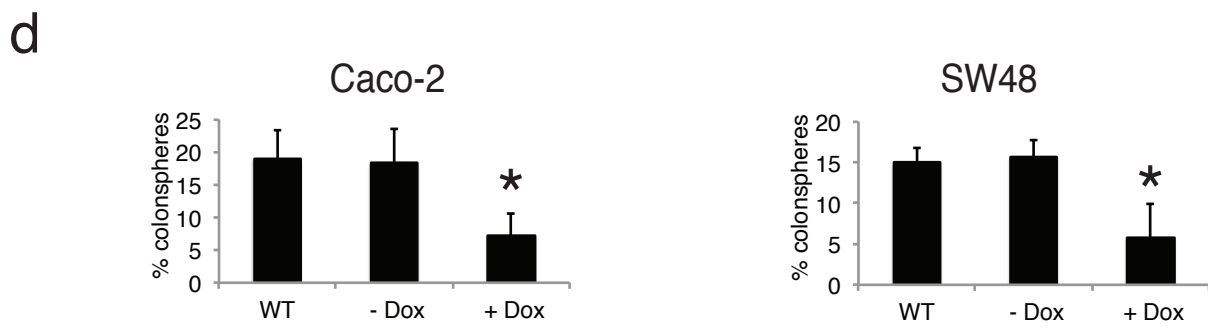
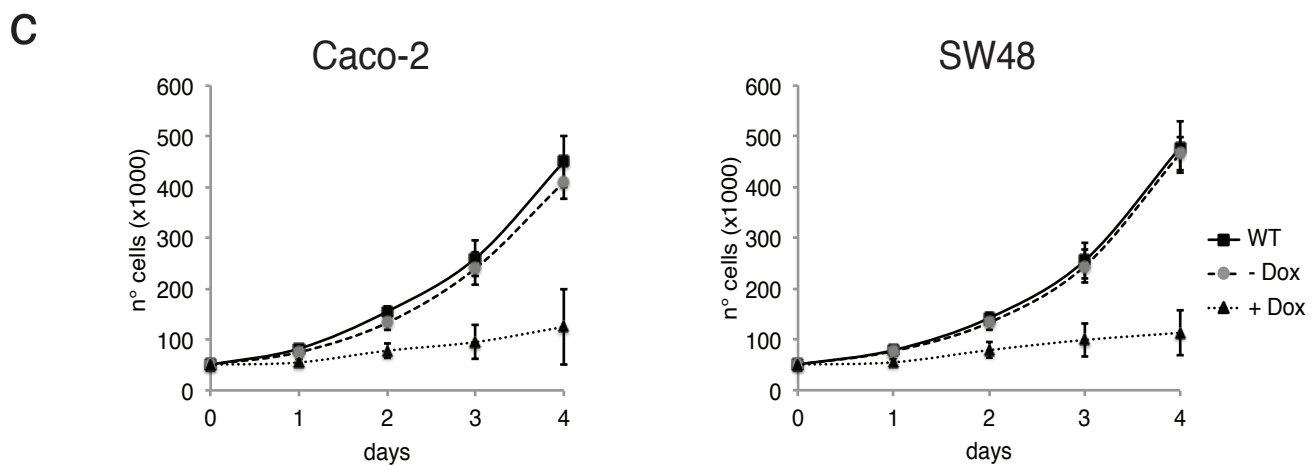
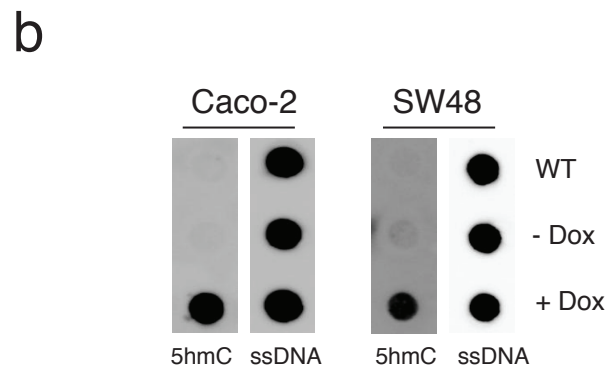
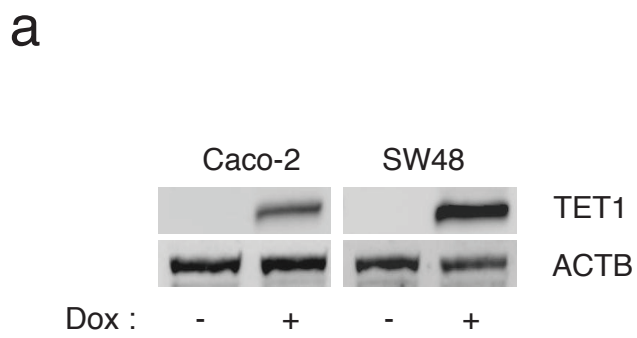
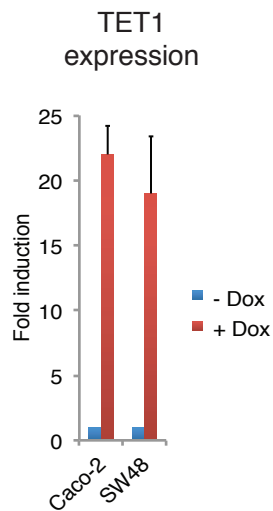
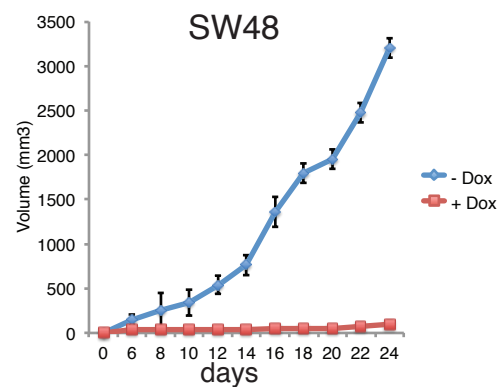
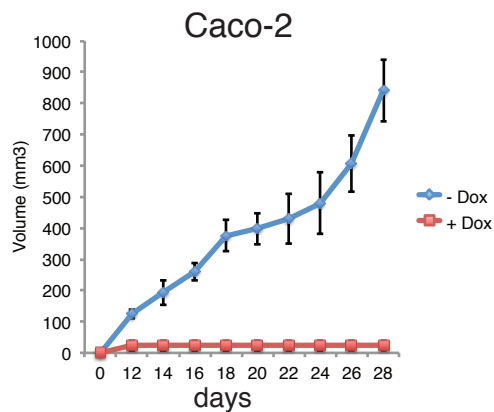
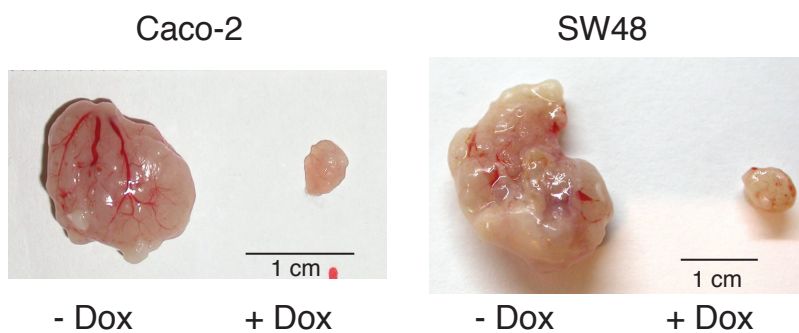
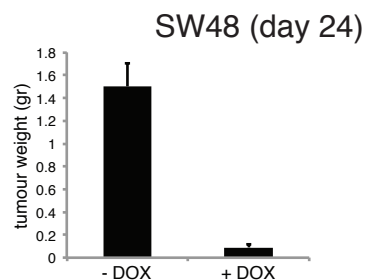
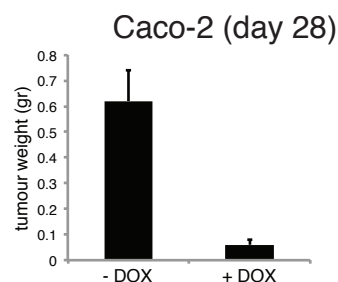
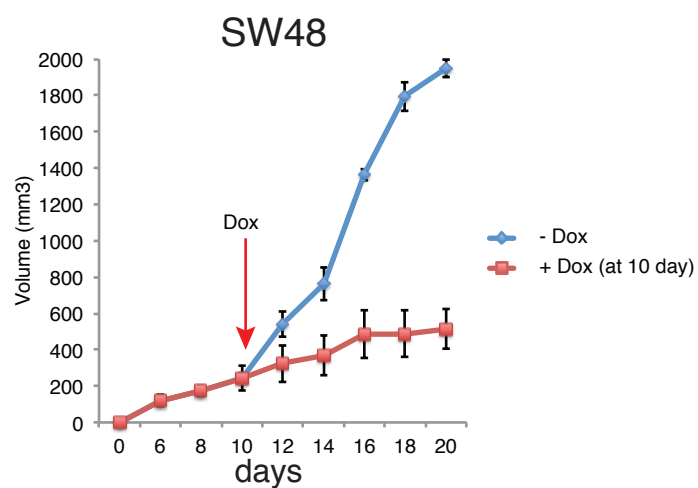
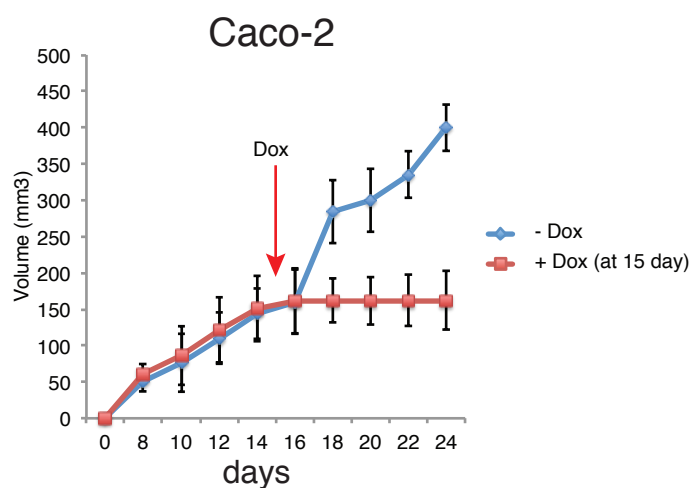


Figure 2

**a****b****c****d****e****Figure 3**

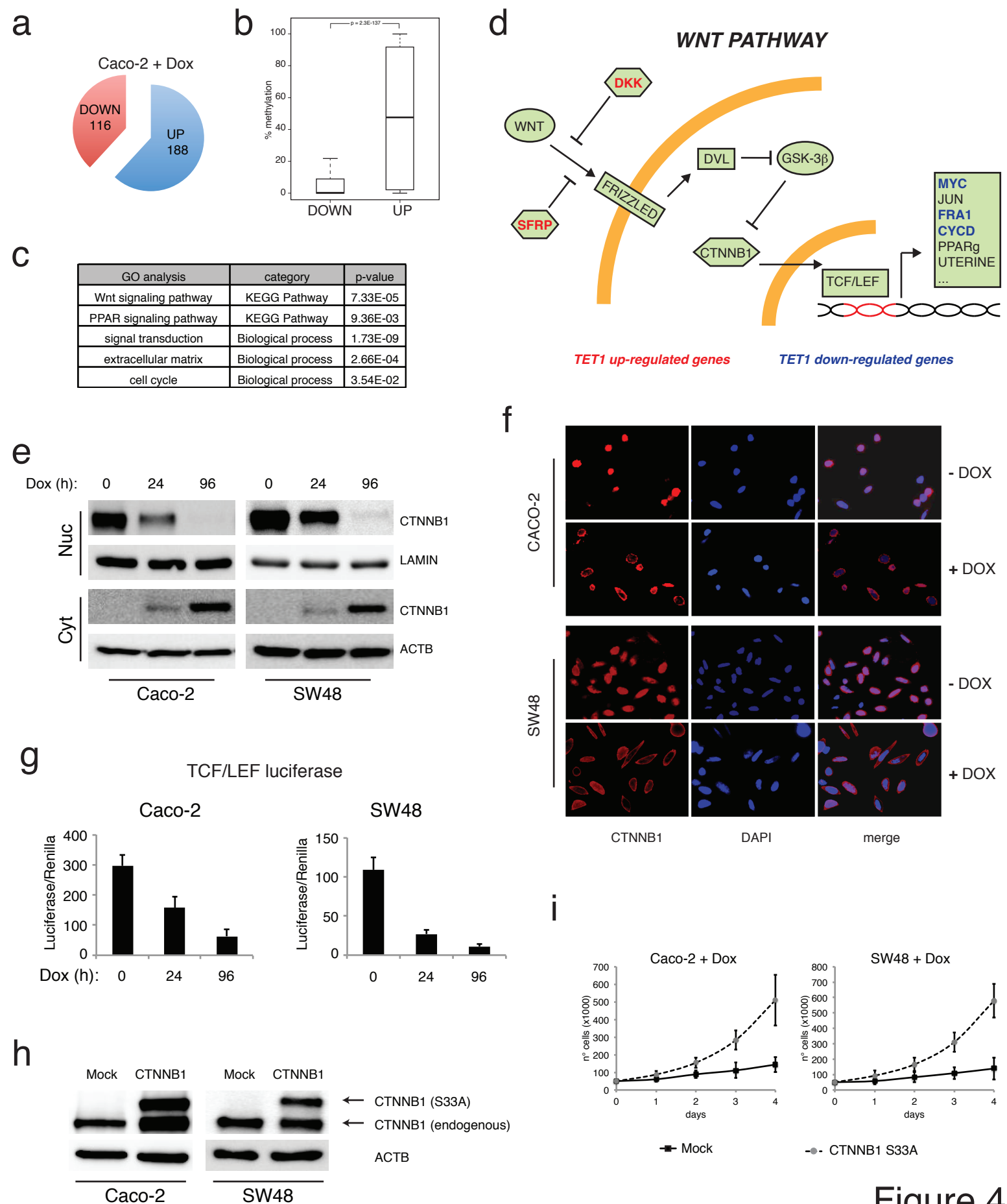


Figure 4

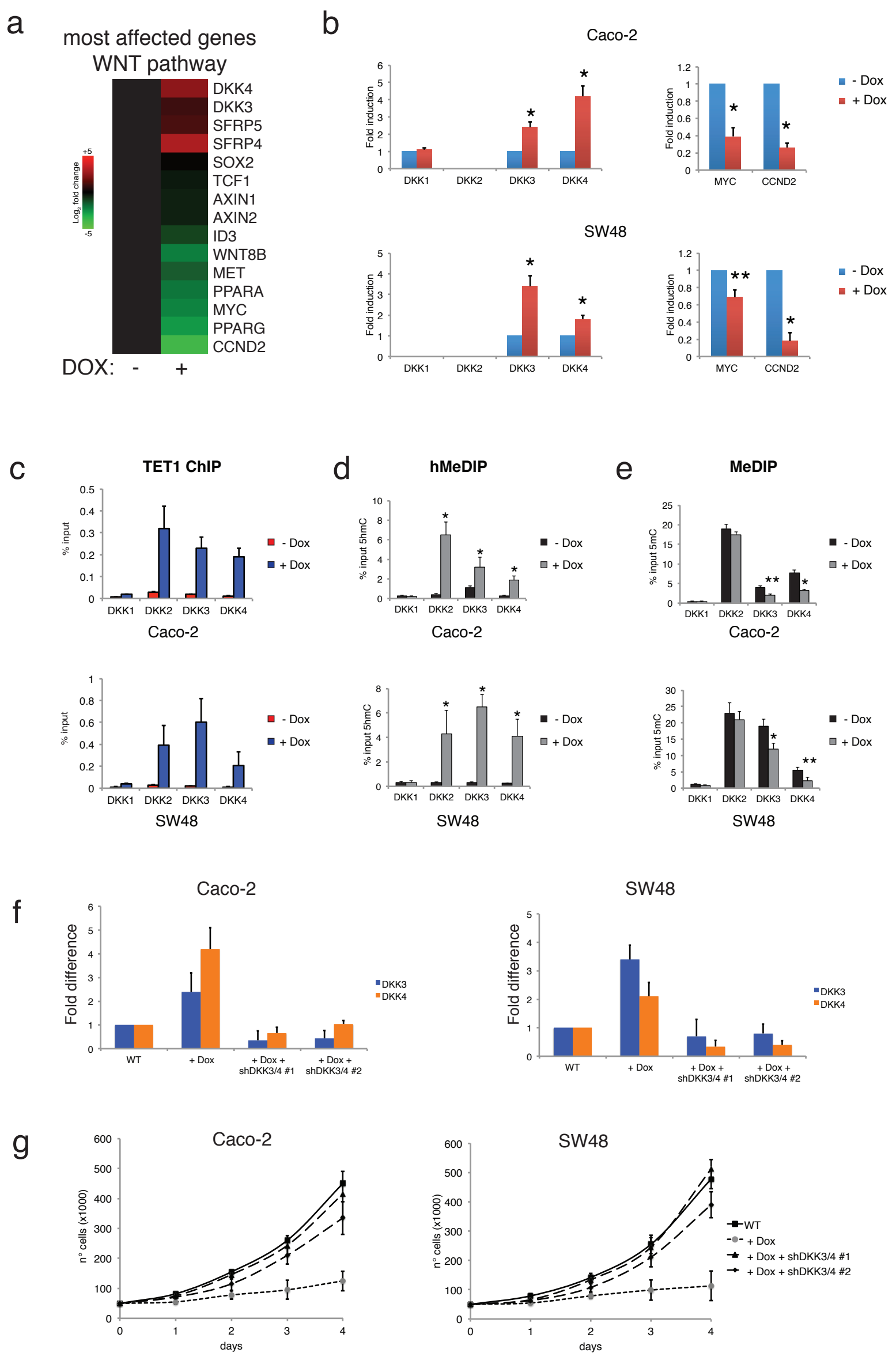


Figure 5